Journal of Power Sources 199 (2012) 1–13

Contents lists available at SciVerse ScienceDirect

Journal of Power Sources

journal homepage: www.elsevier.com/locate/jpowsour

Review

A review of modeling and simulation techniques across the length scales for the solid oxide fuel cell

Kyle N. Grew[a], Wilson K.S. Chiu[b,*]

[a] U.S. Army Research Laboratory, Sensors & Electron Devices Directorate, RDRL-SED-C, Adelphi, MD 20783, United States
[b] Department of Mechanical Engineering, University of Connecticut, 191 Auditorium Road, Storrs, CT 06269-3139, United States

ARTICLE INFO

Article history:
Received 9 July 2011
Received in revised form 4 October 2011
Accepted 5 October 2011
Available online 10 October 2011

Keywords:
Atomistic
Fuel cell
HeteroFoaM
Mesoscale
Multiscale modeling
Quantum

ABSTRACT

Recent advances in computational techniques have allowed the application of computational tools to study heterogeneous functional materials (HeteroFoaMs) in the solid oxide fuel cell (SOFC) from the quantum (sub-atomic) to atomistic to the continuum scales. However, knowledge gained from a particular computational technique can only provide insight at that specific scale. There has been a recent interest to develop a more cohesive effort so that results obtained from models across a particular spatial dimension can be used to extract additional insight across a larger range of length scales. This review article surveys recent progress in the modeling and simulation of SOFCs, and relates them to the relevant physical phenomena and length/time scales. We then proceed to review the various numerical techniques used, and their applicability across the length and time scales.

Contents

1. Background and introduction

Modeling and simulation provides a unique opportunity to assist with the development of materials, components, and practices for next generation solid oxide fuel cells (SOFCs). The methods enhance our ability to comprehend the connections between functional and detrimental behavior and their impact on the cell. However, it is a challenge to treat these aspects across the breadth of time and length scales over which they originate and manifest themselves. This is complicated by the heterogeneous nature of the material structures, which convolutes the challenge of understanding these processes. Modeling and simulation tools can help us to understand these complex interactions. With continued development, these methods may eventually be able to be applied to provide a predictive capability for the design and development of SOFC materials, morphologies/structures, components and systems; however, this remains a significant challenge [1].

As with the heterogeneous functional materials (HeteroFoaMs) [167] themselves, the individual constituent materials, interfaces, and morphologies influence the approach(es) taken. The physical and (electro)chemical conditions of the materials and processes involved can limit the validity and range of applicable approaches. The relevant time and length scales compound the challenge as they ultimately dictate the plausible approaches that may be taken. In

* Corresponding author. Tel.: +1 860 486 3647.
E-mail address: wchiu@engr.uconn.edu (W.K.S. Chiu).

0378-7753/$ – see front matter © 2011 Elsevier B.V. All rights reserved.
doi:10.1016/j.jpowsour.2011.10.010

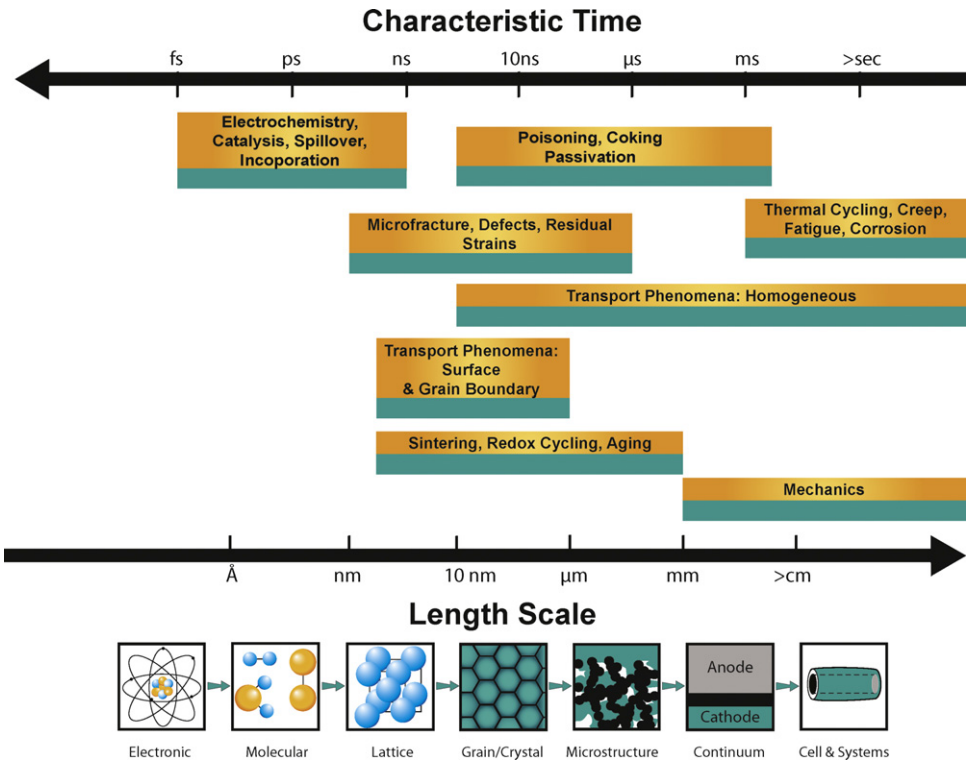

Fig. 1. An overview of the time and length scales characteristic of functional and degradation processes in the heterogeneous SOFC electrode structures. The time and length scales provided are conceptual and are only intended to be characteristic of the scales at which these processes generally present themselves.

Fig. 1, time and length scales representative of SOFC-relevant functional and degradation processes are provided. The interactions for each of these phenomenon originates at the quantum level with the electronic structure of the individual atoms; however, they present themselves in unique observable/measurable ways which can occur at a variety of time and length scales and also provide insights.

Examining Fig. 1, chemical and electrochemical processes are governed by fundamental aspects of the catalytic and electrocatalytic interface. These processes are dictated by the chemical and physical interactions of the molecules and catalytic binding sites to Refs. [2–6]. These processes present themselves at the time and length scales of the electronic interactions of the individual atoms/molecules that determine bond strengths and binding energies of the adsorbed species on up to those of the transport processes which supply them. Fracture and stresses/strains involve the interactions at the lattice level and are directly influenced by features including grain interfaces, phase interfaces and defects on up through the microstructure [7–11].

Homogeneous transport includes mass, charge, and heat transfer, which occurs through the bulk of the pores, materials, and structures. These processes ranges from time and length scales of the materials lattice and structures/features that support them (at the corresponding thermodynamic state) on up to the systems levels [12–15]. On the other hand, surface and grain boundary transport processes must match the length and time scales attributed to the grain structure itself [16–19].

Aging (e.g., coarsening), sintering, and redox cycling tend to occur at scales attributed to the grain structure and microstructure as they involve chemical and physical changes in the materials, interface, and morphology [20–26]. Similarly, poisoning, coking, and passivation involve changes to the materials and interfaces through chemical interactions meaning these aspects also present themselves at the scales of the lattice and grain structure and can impact broader scales [20,27–29]. At the broader time and length scales are aspects like the bulk mechanical properties and component/systems responses to the conditions and history (e.g., creep and fatigue) [11,30–33]. These processes include more fundamental aspects, such as the coefficients of thermal expansion, but are directed toward the bulk components/cells.

The modeling and simulation methods that are applied require comparable levels of precision and control, while also being able to accurately treat the relevant processes and conditions. For example, specifics of the mechanisms attributed to the electrochemical reaction kinetics may be studied by using density functional theory (DFT). Various processes and pathway(s) can be determined by mapping the corresponding potential energy surfaces, with saddle points corresponding to transition states. However, semiconductors and materials with highly correlated electronic structures require more rigorous approaches, such as DFT + U and quantum Monte Carlo methods, because the exchange correlation functions of traditional DFT methods do not provide the necessary accuracy [1,34]. This can be relevant to transition metal oxides and ceramics, like those often used in the SOFC. Aspects requiring the incorporation of longer range and non-periodic effects can also be difficult, especially as finite size effects including heterogeneities and morphologies come into play. Processes involving chemisorption, vacancies/defects or impurities, and electrochemical polarization are examples, which generally require embedded cluster methods. Accurate partitions are required to couple phenomena, which are difficult and specific problems in their own right; however, again necessary [34]. Insufficient treatment of these aspects can result in un-reliable predictions in mechanisms and properties attributed to the system.

At broader scales, there are parallels in the methods for the modeling and simulation of transport phenomena, where aspects such as the inclusion of the appropriate physical phenomena when the length scales approach the mean free path [13–15], space charge

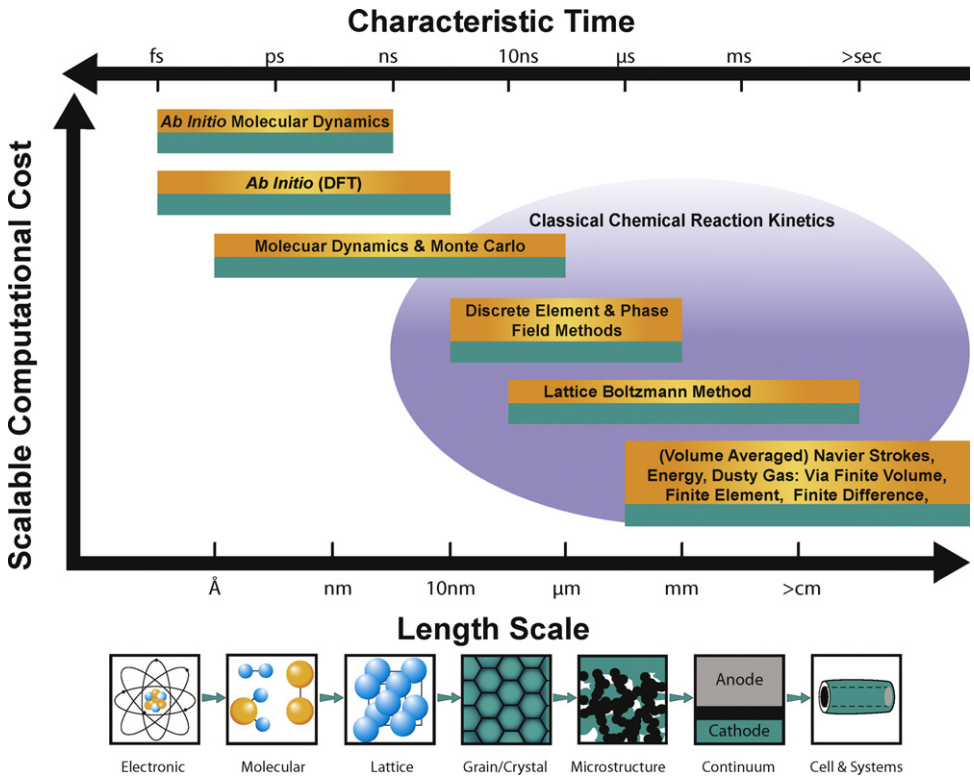

Fig. 2. Several of the modeling and simulation methods applicable for the SOFC, where the scalable cost is plotted versus the time and length scales that can be resolved. Computational cost represents relative trends.

effects [35–38], the presence of poisons [27,39–54], and so on can have similar influences. Scenarios like the presence of unexpected secondary trace elements and poisons signify a limitation; theoretical approaches require an accurate understanding of the physical conditions germane to the problem at hand. If unknown traces of poisoning elements/species leach into the cell from the surrounding environment and/or balance of plant, their contributions and effects cannot be accounted for. This highlights the continued importance and need for detailed experimental efforts for checking and validating our understanding as well as defining the constraints of our physical problem.

2. Approaches to modeling and simulation

The typical scientific approach to research and development either relies upon trial and error, the so called Edisonian approach, or it relies upon the maturation of the scientific understanding of the relevant materials properties, thermodynamic properties, physics, chemistries, and responses of the system through systematic exploration. Individual aspects of the system are separated and studied to help refine this understanding. This has often been accomplished by means of tedious experimental effort. Modeling and simulation across the time and length scales provide unique opportunities to understand properties and phenomena that are inaccessible and difficult to address with experimental effort, or have inseparable multifaceted interactions. As noted in Fig. 1, discrepancies in the length and time scales of these functional and degradation processes exemplify these modeling and simulation needs for understanding the porous structure and its constituent materials, interfaces, and morphology. Many of the typical approaches are described in Fig. 2, which presents the modeling or simulation methods' relative computational cost (not to scale) versus the approximate characteristic time and length scales that they can resolve. Comparing Fig. 1 to Fig. 2, it is apparent that no single method is suited to studying the full scope of challenges.

Fig. 2 demonstrates that different approaches are required to capture different time and length scales. While aspects including the relative domain size and durations can affect the computational cost of a study, the cost tends to decrease with increasing time and length scales. This is a general observation that accounts for the scalability of the approaches (i.e., parallelization), but should not be taken as a universal rule. At the most fundamental scales are *ab initio* Molecular Dynamics (AIMD) and *ab initio* methods, such as DFT, examine the electronic structure (quantum) of the respective atoms and the corresponding interactions [1,34,55,56]. AIMD uses the resulting potentials and forces to calculate the dynamics of the atomic and molecular interactions. The expense of these methods is tied to the time scales of the electronic structure of the atoms relative to those of the atomic/molecular dynamics, as well as the numerous interactions between atoms and molecules. To a lesser degree, this holds for Molecular Dynamics and Monte Carlo approaches, which use predetermined force fields to dictate molecular interactions in place of detailed calculations of the electronic structure [56].

Discrete element and phase field methods are often used to study the formation and evolution of grain and microstructure in such systems. This may include aspects such as sintering, compaction, and aging resulting from the non-equilibrium thermodynamics in such systems [57–59]. Transport phenomena in discrete microstructures, may be captured using methods built upon the Boltzmann transport equation, such as the lattice Boltzmann method (LBM), which is scalable and enables the use of a low resolution, regular mesh [60–62]. The underlying Boltzmann equation is applicable from free molecular to the continuum scales; however, LBM is typically formulated so that it recovers the Navier–Stokes and energy equation. Empirical and rigorous mathematical approaches have been attempted to extend its applicability to finite Knudsen numbers [63–65]. More traditional methods, such as those using the Navier–Stokes equations, energy equation, dusty gas equations, as well as Navier's and related mechanical

constitutive equations may also be considered [12–15,66,67]. These methods are typically discretized with finite element and finite volume method, which can be difficult to mesh in complex structures. Therefore, these methods are often used for volume averaged representations of the materials/system (i.e., homogenized). The typical numeric methods used to solve these equations (i.e., finite element, finite difference, and finite volume) may also be used to solve other interactions and processes as long as they are properly represented in the form of systems of partial differential equations.

Chemical and electrochemical kinetics are typically implicitly included in atomistic and molecular methods; however, they must be determined and explicitly accounted for at broader time and length scales. Both heterogeneous and homogeneous kinetics are typically described as being stiff, indicating a disparity of time scales involved [4–6]. While the underlying interactions follow quantum to molecular time and length scales, the equilibration process can follow and/or dictate transport processes indicating that they can change over a wide range of time and length scales. Solution of such a mechanism is repetitive, can dictate time steps permissible for the modeling of other coupled processes, and become prohibitively expensive to evaluate as the complexity of the mechanism increase.

2.1. System, cell and electrode level approaches

Systems, single-cell, and electrode-level SOFC modeling constitute one of the broadest efforts to represent the SOFC and its function with theory. These approaches are often broken down into steady state or transient models and can range from zero to three dimensional descriptions of the system, cell and/or electrode. These approaches are often used to study the effects of changes in component design/materials, fuel and oxidant, conditions, and/or coupling between processes. Specific aspects of the system, cell or electrode, such as cell performance, fuel utilization, stresses/strains, dynamic response, and/or thermal signatures and conditions are typically the focus of such efforts.

To describe interactions in such a system, conservative continuum theory, such as Ohm's law, Fick's law or a Stefan–Maxwell or Onsager's based multi-component theory, Navier–Stokes equations, energy equation, Navier's equation or a related small deformation continuum mechanics theory, is often used with the inclusion of non-continuum principles as applicable. Non-continuum principles can become important for aspects including the description of diffusive mass transfer because of the temperature and length scales involved (e.g., Knudsen flow). These aspects are often treated with the use of the dusty gas equations [15]. Cell potentials are often dictated by the Nernst equation with activation overpotentials calculated via the Butler–Volmer equation. In general, finite elements, finite differences, finite volumes, collocation methods, and/or marching schemes are used to discretize and solve the governing equations.

This is representative of the three-dimensional models published by Khaleel and coworkers, which couple transport and electrochemical processes within SOFC single-cells and stacks [68–70]. Finite element analysis was used to solve a Navier–Stoke's based description flow, along with the energy equation to account for heat transfer in the form of conduction and advection [68,69]. An electrochemical model with the Butler–Volmer equations was used to calculate the overpotentials associated with the oxidation and reduction reactions, along with the corresponding heats of reaction. The effects of fuel and oxidant flow configurations and cell layout on dynamic and localized temperature distributions, concentrations, and pressures have been examined with this approach.

A key consideration for this approach is how the heterogeneous electrode structure should be represented and its influence on the functional processes. Empirical factors, such as a porosity–tortuosity factor, exchange current density, TPB length, catalytic area, percolation probability or effective media approximations, permeability coefficients, mean pore/particle size, and area specific resistances, are used. These parameters may be obtained using a variety of approaches including fitting and estimating from independent experimental measurements. As will be discussed in more detail, theoretical and conceptual representations of the microstructure are also commonly used to estimate these types of parameters. The underlying premise of this approach is to simplify the conceptual construct so that the cell's physical behavior and responses may be replicated. Then, a full gamut of variations occurring within the cell can then be obtained and the model may be validated using experimental data. Parametric variations in the physical cell description or the empirical parameters can then be used to optimize aspect(s) of the cell design.

The importance of the microstructure's description has been noted by Kee and coworkers [71–73]. Cell-level modeling efforts provide a valuable tool for obtaining these types of details; however, making adjustments to the various cell components based on these global models may be challenging. The methods implicitly assume that the complete sets of appropriate physics are being considered with sufficient fidelity to capture the spectrum of relevant processes. Complex heterogeneous structures are treated on a volume averaged (homogenized) basis, assuming consistency. While this provides an effective means of making it tractable to solve, disconnects can exists between the identification of target values for these empirical parameters in these models and how the heterogeneous structure may be changed to achieve the target. More specifically, how this may be done without having other deleterious effects.

An interesting and unique attempt to address some of these challenges has been taken up by Bessler and coworkers [74–77]. Transport and reaction models that calculate electrochemical impedance spectra have been developed so that electrochemical and transport contributions incorporated in the cell's description can be translated into the frequency domain. This allows contributions within the physical and electrochemical processes, as well as those related to the description of the microstructure, to be separated based upon their contribution in the frequency domain. Comparing to complementary experimental electrochemical impedance spectroscopy data provides confidence in the details extracted. The details ascertained from the impedance modeling can then be used to simulate cell transport and polarizations [77,78].

A rather comprehensive cell-level approach has been reported by Kee and coworkers, which involves the direct internal heterogeneous methane reformation reaction kinetics developed and incorporated into two- and three-dimensional transport models of planar and tubular SOFCs [71,79–82]. Elementary reaction kinetics describing internal methane reformation processes have been assembled for this effort and are numerically solved with a damped-Newton method for nonlinear systems of equations using the pseudo-steady state approximation. Mass transport in the porous electrode is treated with the dusty gas equations, which is coupled with principles of species, electronic and ionic charge, continuity, momentum, energy conservation within the system [71,80–86]. An extensive effort has been placed on validation of their reaction kinetics model using custom flow cell with a isolated Ni–YSZ anode and mass spectroscopy probes to measure changes in chemical compositions, which showed their kinetics were able to reproduce the experimental measurements with considerable fidelity over a wide range of flow, composition and thermal conditions corresponding to SOFC operation [87]. Additionally,

direct internal reformation cell models exhibited agreement with SOFC polarization experiments, including for various methane feed compositions and conditions [71,80–86]. Results from these works have provided insight into the nature and extent of heterogeneous internal methane reformation in the SOFC. In collaborative efforts with Barnett et al., this approach has been extended to study coking processes [86]. This has helped to spurn design developments, such as anode-oxide support layers to enhance chemical stability with hydrocarbon-based fuels, where the models were able to provide the proof of concept and design input [88].

Among the challenges confronting the heterogeneous SOFC structures is to maintain mechanical integrity. Elevated temperatures and corresponding gradients cause the materials to undergo thermal expansion. Differences in coefficients of thermal expansion (CTE) between the constituent materials and layers of the cell result in thermal stresses. Thermal stresses can cause cracking within the microstructure or even delamination and other catastrophic failure [11,30,32,89–91]. These effects are most pronounced during the transient period associated with thermal cycling and load following that can induce large internal temperature gradients [31,32,92,93]. They may be further compounded by stresses induced by the mechanical constraints from the cell's seals and packaging [31,94], volumetric changes during redox cycling [32,95] and poisoning [54].

In many regards, efforts to simulate the thermal stresses at the system, cell, and electrode-levels are similar and complementary to the performance models. These models require that the materials and structures be treated on an effective, homogenized basis. Finite element analysis is often used to solve the thermo-elastic problem (e.g., Energy and Navier's equations) along with the required constitutive equations, which assume a linear material response according to the principles of small and elastic deformations [30,32,90,93,94,96]. Challenges to these approaches include the (i) treatment of the often brittle material as elastic or quasi–elastic, (ii) determination of the baseline mechanical properties which can be strongly dependent upon microstructure and composition, (iii) development, coupling, and validation of a detailed thermal-fluid and chemical models, (iv) identification and implementation of appropriate boundary conditions, and (v) validation of the models. Validation can be difficult because system and operational aspects play a prominent role; however, methods including nanoindentation [33] and X-ray diffraction (XRD) [97] have provided some new capabilities.

Attempts to extend the stresses/strain fields calculated by the thermo-mechanical and degradation models have also been used to predict crack initiation and propagation dynamics [10,11,30,89,92]. Crack propagation modes, trajectories, stress intensity factors, and interactions resulting from residual stress and strain fields must be considered [10,89]. The intermittent and unpredictable nature makes it a formidable challenge to assign parameters and validate results. Weibull statistics have been incorporated to predict failure probabilities resulting from mechanical degradation mechanisms [11,30–32,90,92]. A probabilistic measure of failure provides a measure of the influence of different aspects of the heterogeneous structure and cell design. These principles have been used to demonstrate limits on thermal gradients [32], cycle steps and conditions [32], contact pressure and flow conditions [31,32], and functional grading of the electrode structure [90]. However insightful, these analyses can be difficult to validate without including far-reaching experimental programs.

This sample perspective of the system, cell, and electrode level models that have been reported within the SOFC community provides detail on the nature and impact that such approaches can have. At these time and length scales, more extensive reviews on the dynamics [98], aspects of operation [99], and modeling approaches [99,100] are also widely available.

2.2. Discrete morphological models

We move from cell level to discrete *model* representations of the heterogeneous structure's morphology. This class of models are described as morphological, meaning that they consider either an (i) discrete idealized or (ii) artificially generate representation of the heterogeneous structure. These systems are used to test microstructure properties and/or to test hypothesis regarding the effects of properties selected during manufacturing.

Discrete idealized structures may be considered as those where physical packing of the microstructure is fixed. Percolation theory, which uses the coordination of electrode and electrolyte "particles" in a presumed lattice arrangement, is consistent with this definition [73,101–104]. A contact angle that dictates the constricted contact between discrete particles is selected as an input to these models. However idealized, the model provides an estimate of the reduction in conductivity due to the organization of the homogenized microstructure. The effect of the structure on the overall conductivity can be calculated, along with estimations of the electrochemically active three-phase boundary (TPB) length and interfacial areas between constitutive particles on the basis of coordination number, particle sizes, volume fractions, and average inter-particle contact angle.

Results from percolation theory approaches include limitations on volume fractions and the contributions of unique particle sizes to TPB length and degree of percolation for electronic charge, ionic charge and mass transfer processes definition [73,101–104]. Many of the studies discussed use percolation theory to assign properties to the microstructure. Percolation theory is widely accepted because of its ability to reduce the complex heterogeneous construct to a few descriptive parameters that follow established trends, including validation versus experimental area specific resistance measurements (ASR) for unique electrode compositions [101,104]; however, it is inherently limited to describing these structures as highly idealized constructs. Bimodal particle distributions, commonly used with the electrolytic material in the electrode structures, are difficult to treat. Even though microstructure properties can be estimated, there may still be significant variations within actual structures.

A second idealized approach was reported by Virkar and coworkers [105,106]. Rather than using discrete coordinated particles, Virkar and coworkers considered electrolytic fins with electrode particles placed on the periphery of the fin to provide the electrochemically active interfaces. The electrode structures were treated as homogenized media, with effective properties that are descriptive of the microstructure. These fins were then used to calculate effective charge transfer resistances on the basis of an ideal intrinsic charge transfer resistance and descriptions of the microstructure. Effective charge transfer resistances were found to be higher for thin electrodes and then decrease once a critical electrode length was reached. Finer particles also decreased effective charge transfer resistances [105,106]. In these studies, the effective charge transfer resistance calculations were compared to corresponding experimental measurements where the electrode thickness was varied.

In a similar approach, Nelson et al. treated the structure as an electrochemical fin to better understand charge transport within a conceptual structure with an allowance for variable cross sections [107]. While the approach includes empirical treatments of particle size and details regarding the sinter quality, it enabled distinct charge transport regimes within the SOFC electrode to be understood in terms of how they relate back to the microstructure. The study was validated by comparing polarization resistances for both electrodes of different thicknesses as well as those that were well and poorly sintered, resulting in different aspects of inter-particle contact. An interesting result of this approach was

the analog to traditional heat transfer "fin efficiencies" which provide an effective measure of the quality and performance of the structure relative to if transport and electrochemical reaction.

An alternative approach is to artificially generate a structure that may be used to represent a heterogeneous material that may be representative of the heterogeneous electrode structure. These types of methods rely on stochastic procedures. In works by Sunde, Monte Carlo methods were used [108–110]. Two approaches were shown by Sunde. The first used random number generators to populate a cubic lattice with electrode, electrolyte, and pore particles with some pre-determined volume fraction [108]. In a second more rigorous approach, the random placement of spherical particles was used [109,110]. Additional particles were randomly brought in and added to a three particle cluster of spheres in hard contact. Particle contact was fixed as a discrete point. Overlap for both approaches, representative of the sinter process, was treated by allowing all particles to simultaneously expand until an adequate degree of overlap was achieved. Sunde treated the structure as a random resistor network and use Kirchhoff's current laws to calculate the effective properties of the microstructures. For validation, results were compared to independent conductivity measurements.

Following Sunde's efforts, Martin and coworkers tried to improve upon the accuracy and physical relevance of these types of methods through the use of a discrete element method (DEM), which uses Monte Carlo methods to generate an initial structure followed by a simulated relaxation process to represent the actual processing steps that the heterogeneous SOFC electrode architecture undergoes [59,111–113]. This approach, first used to describe particle interactions during compaction [59], predicts the evolution of particle trajectories according to Newton's laws of motion. Inter-particle collisions are treated during relaxation. Particles are not allowed to overlap during relaxation; however, they are subjected to a volumetric expansion to obtain the desired contact angle that is deemed representative of the sinter process in a manner to that of Sunde. A recent study compared DEM, standard Monte Carlo, and percolation theory predictions, found comparable predictions of coordination number, percolation probability, TPB lengths, and effective conductivities over a range of volumetric compositions [114].

A unique stochastic approach, designed for the reconstruction of random heterogeneous and multifunctional media, has been developed by Torquato and coworkers [115–119]. Torquato's approach assumes that real structures can be used to ascertain correlation functions that represent the dispersion and interactions of the unique phases within a multifunctional heterogeneous material. If a correlation function adequately describes the heterogeneous structure, it may then be used to produce an infinite number of artificial structures that are statistically representative of the original. This approach could allow an infinite number of permutations of a valid microstructure to be numerically produced, which is of great use when trying to understanding the nature and role of the structure.

As a part these efforts, Torquato has shown procedures to reconstruct random, multi-phase, anisotropic heterogeneous media from morphological descriptions of a base-line system [115]. This is accomplished using an *n*-point correlation function to provide the degree of morphological information as needed. Reconstruction of an isotropic ceramic-metallic composite (cermet) was demonstrated by using orthogonal sampling with a two-point correlation function that did not exhibit short range order effects. However, in addressing uniqueness, variability between reconstructions with different initial guesses is noted as a direct result of finite size effects [117]. This was later identified as a more significant challenge, when a 2-point correlation function was found to work well for reconstructing heterogeneous materials with a single-scale structure, but was not as well suited to a multi-scale random media [118,119]. This suggests that challenges remain for using this approach with broader multifunctional heterogeneous materials, which can contain hierarchical structuring with the length scale of features spanning several orders of magnitude. Despite these challenges, the concept of statistical correlation to actual structures is quite interesting and unique.

2.3. Micro- to nano-scale approaches

The consideration of discrete heterogeneous nano- and microstructures within the context of modeling and simulation can provide unique details. In many instances, details resolved at nanometer length scales (e.g., grains, grain boundaries, inclusions, phase-interfaces, contact/dihedral angles, and pore cross-sections) can be considered while also maintaining long-range order (i.e., properties become volume-independent) that is often found in the vicinity of several to tens of micrometers. While this requires the use of representative volumes, it permits the unique functional processes, and their coupling to the discrete heterogeneous structure, to be captured. The physics and chemistry must be understood and defined prior to simulation; however, the influence of the heterogeneous structure on these processes can be accounted for on a non-empirical basis with confidence in these descriptions.

There have been numerous groups working at the levels of the heterogeneous structures at the nanometer to micrometer length scales. Reifsnider and coworkers examined the relative contributions of grain boundary diffusion to the ionic conductivity of ScSZ [17] using input from a scanning electron microscopy micrograph, where elemental phases and individual grains and grain boundaries could clearly be distinguished. This study was performed to highlight the importance of the individual grains and structure at nanometer length scales for this functional heterogeneous structure. Approximately 12% difference in effective conductivity was identified due to the consideration of grain boundary diffusion mechanisms.

The study by Reifsnider and coworkers highlighted the importance of the grain structure at these levels. Efforts by Zhao and Virkar took a related approach, but with unique considerations [37]. These considerations included accounting for the morphology of the inter-particle necks and the contributions of discrete grain boundaries to the space charge regions that promote defect stacking and can assist and/or hinder the bulk conductivity. Zhao and Virkar considered the conductivity of porous SDC that was made via standard powder compaction method and using NiO-SDC sintering. The NiO was subsequently reduced to Ni and leached with acid. Porosity of the samples was held consistent; however, the acid-leached SDC sample had an experimentally measured DC conductivity that was up two orders of magnitude larger than the compacted sample. Using an analytic development, these discrepancies were attributed to the inter-particle neck size, which were clearly different for the unique methods. In addition to the inter-particle neck sizes, space charge regions contributions were considered for both dense and porous samples. Space charge contributions were identified as significant in porous samples with small inter-particle necks.

The contribution of space charge regions, or the depletion and/or stacking of electronic and ionic defects near interfaces in solid state devices, is a topic that has been well studied due its importance to nanostructured systems and its corresponding interfaces [38,120–125]. Maier et al. have established an expertise in this area, forming both analytic and numeric approaches to describing the effects of space charge. This includes aspects of the all-important defect chemistry in the interfacial region [121–123] and the associated thermodynamics [124]. These approaches have been extended into chemical transport [38,121] and equivalent circuit models [125] capable of describing discrete structures, to understand the

geometric morphological affects [38,120,121,123,124]. The importance of these contributions, as recognized by Zhao and Virkar [37], is that they can have a very real contribution to the overall behavior of the system and are a key aspect into understanding this behavior. Further, a relatively broad class of test materials coined heterostructures has shown anomalous ionic conductivities as the space charge regions (i.e., Debye length) are confined in controlled lattices, which have been validated using a wealth of Arrhenius conductance measurements with unique structures [120]. These effects become more pronounced as these conductions zones are further confined. The role of lattice strain in the vicinity of the interface may also be questioned, among other things. However, the measurement of drastic increase in ionic conductivity via exploitation of these principles point to their potential impact [126]. Certainly, these principles can be implemented in stable, functional heterogeneous materials where they can enhance conductive transport, including at lower temperatures which offer a number of cursory benefits. Such an undertaking requires both advances in scientific understanding of the physical processes occurring in these structures to relate these principles into rational model-based design.

LBM, a scheme using the discretized form of the Boltzmann equation, represents a simplified kinetics approach to describing transport phenomena in a discrete heterogeneous structure [62]. LBM uses a velocity-space representation of the fluid, using a probability distribution function (PDF) to provide a statistical representation of the fluid and its interactions. PDF moment closures are used to recover macroscopic fluid properties including concentration (or density) and fluxes (momentum, energy). Molecular interactions, which dictate the fluid's viscous and/or diffusive processes, are treated with a Bhatnagar–Gross–Krook (BGK) collision operator(s) to relax the system versus a Maxwellian distribution. Because it is rooted in Boltzmann statistics, LBM provides a more fundamental description of molecular interactions than the Navier–Stokes equations, which can be exactly recovered [62]. Efforts to extend the LBM formulation through the transition transport regime to finite Knudsen numbers have also been undertaken [63–65]. Regular meshes at rather low mesh density can be used with considerable fidelity, which is a substantial benefit for handling the complex features observed in actual structures that can make traditional meshing schemes nearly intractable. Transient relaxation toward equilibrium occurs as an explicit time marching process. The PDF at each lattice point is only dependent upon its nearest neighbor lattice points, which are updated during a streaming process occurring at every time step. Consequently, the explicit method provides nearly linear scalability with parallelization.

LBM has been used to perform a variety of numerical simulations within the SOFC community. Chiu and coworkers have used LBM to study mass and charge transport in the heterogeneous structure of the porous Ni–YSZ cermet SOFC anode [64,127–135]. These efforts have included the development of a N-component multi-component LBM approach, capable of simulating continuum [127] and non-continuum [64] diffusion processes; which were subsequently applied to 2D conceptual electrode structures to ascertain the links between porosity, tortuosity, and concentration polarizations [128]. Initial efforts in these studies were validated using independent analytic methods and experimentally measured concentration polarizations. Asinari et al., used LBM with granulometry theory based scanning electron microscopy micrographs of actual samples to simulate transport phenomena in a reconstructed 3D porous Ni–YSZ cermet anode to calculate localized fluxes are shown and macroscopic tortuosity, as a function of position in the anode [136]. The efforts of Chiu et al. and Asinari et al. represent some of the first efforts to utilize reconstructions of actual heterogeneous electrode structures to perform discrete transport simulations.

Mass and charge transfer were also explored by Chiu and coworkers in actual SOFC anode microstructures, obtained using tomographic reconstruction of advanced transmission X-ray microscopy data and supplemented by sphere-packing generated structures [130,131,133,134]. Nonlinearities and variations in pore-scale concentrations and potentials were observed in these studies, resulting from the complexity of the actual structure. The power of these methods lie in their capability to link morphology to their contributions to transport and interfacial phenomena, which were captured when an explicit quantitative coupling was made between the respective grain "particle sizes" and their contributions to transport losses [133,134]. These details were captured in conjunction with quantitative descriptions of the size distribution, interfaces, connectivity, and tortuous nature of the morphology to demonstrate the connection between these morphological descriptions and the relative performance [130,131,133,134,137]. Shikazono et al. demonstrated the use of FIB-SEM reconstructed RVEs of a thin porous Ni–YSZ cermet anode to incorporate full details of polarization, including electronic and ionic charge transfer processes [138]. The Butler–Volmer equation was used to represent electrochemical oxidation and the electronic and ionic charge transfer processes were on the basis of gradients in their chemical potential. Following validations using experimental measurements of button cell anode polarizations as a function of current density with different inlet H_2 concentrations, localized concentrations/potentials, fluxes, and current densities were identified. These studies demonstrated the considerable nonlinearity of the overpotential—as is primarily dictated by the resistive electrolytic phase.

As demonstrated by the Shikazono et al., one of the many utilities of LBM is its ability to capture reactive transport. These processes are especially important in the SOFC, because they couple the discrete functional processes through the heterogeneous structural interfaces. Additional studies have been performed by Chiu et al. to explicitly link elementary kinetics mechanisms describing detailed electrochemical oxidation kinetics [129,132] and detailed heterogeneous internal methane reformation kinetics [129,135] to the transport processes to better understand the effect of this coupling. These approaches showed the sensitivity of the coupling, role and importance of the discrete microstructure, and unique kinetic regimes of reactive transport in these systems. Such trends are characteristic of a multi-scale coupled system.

Phase field modeling is also an important tool that has shown considerable insights into the aging and the evolution of the SOFC microstructures, which occur over broad time scales. These models can describe microstructural evolution due to processes like Ostwald ripening [139], precipitation reactions [140], and heat treatment and thermally induced coarsening [141,142], among others. Empirical inputs and/or calibration are typically required as not all of the degradation mechanisms, rates and processes are quantitatively known due to the time scales involved.

This is consistent with a work by Kim et al., who present a phase-field modeling approach for the SOFC anode [143]. Aging of the SOFC anode microstructure was described using the Cahn–Hilliard equation, which is calibrated with experimental input to kinetic parameters. The Cahn–Hilliard equation in just one approach, as analytic, boundary integral and general phase field approaches are also available. The Cahn–Hilliard equation is used to describe continuity of material flux due to differences in free energy across an interface. Sinusoidal representations of phase interfaces in equilibrium were used and curvature corresponding to particle sizes provides additional free energy contributions. Cell performance was described with homogenized empirical parameters in representative volume elements. A series of representative volumes were used to discretize the anode thickness and the associated mass transfer, charge transfer, and phase field representations were solved using

a finite difference method. Phase-field variables were assigned to each RVE and changes in particle diameter and TPB length were studied over 100,000 h of operation. Changes in Ni particle diameter matched experimentally measured values obtained over 3000 h of cell operation. The experimental measurements were taken from the literature, which consisted of characterization made using line intercept methods on micrographs of sectioned samples.

In a work demonstrating the capabilities enabled by having physical representation for the 3D microstructure, Chen et al. used FIB-SEM reconstructions of the Ni–YSZ cermet SOFC anode as an input to a phase field model [144]. For this effort, the group studied the coarsening of Ni in this system with aging and more specifically the implications of assumptions regarding the mobility of the secondary phases and correlate phase field results to physical measurements of the microstructure, such as changes in electrochemically active TPB length, inter-phase contact area, and tortuosity. While this particular study did not perform detailed validations, these are properties that have been measured in the SOFC by others using FIB-SEM and X-ray based tomographic methods [131,133,134,137,145–148]. Interestingly, Chen et al. [144] note the importance of the contact angles on the aging behavior, with a reduction in the Ni–YSZ contact angle decreasing reconfiguration within the microstructure. This is not unexpected, as the contact angle dictates the force of adhesion between the phases and the energy that is ultimately required for reconfiguration; however, the ability to correlate and map these effects between the theoretical model and physical observations in the actual system promise to greatly improve the fidelity and capability of these phase field methods and provide access to suggest materials and design changes.

Besides aging and microstructural evolution, there is merit to considering the mechanical aspects of the grain-level structure. There are some considerable challenges to such an effort, such as applying boundary conditions, accounting for residual stresses, and resolving an accurate and tractable thermal model if aspects such as thermal expansion want to be considered. With a few exceptions, these types of challenges have significantly limited the work done in this area. Micromechanical models describing fracture in heterogeneous and grain-level systems are available and typically limited to cohesive fracture in brittle materials [9,149]. These approaches again use RVEs, where actual grain morphologies are required. Within the RVE, finite element descriptions of an anisotropic elastic media are used with cohesive interface elements along the crack front. As noted in these studies, the difficulty lies in validating the models and approaches as they inherently occur at relatively random time and locations in the actual system. Aspects, such as crack patterns and velocity histories can provide insight, but the challenge remains formidable. Still, the benefit of such models is being able to predict constitutive material/structural properties both with and without defects.

Possibly a more tractable example and demonstration of changes in the mechanical behavior of the heterogeneous electrode structures has been demonstrated by Liu et al., where the effect of phosphorous poisoning on the structural integrity of the cell was explored [54]. Finite elements are used to discretize the linear elastic and constitutive equations within actual 2D SEM micrographs of sectioned porous Ni–YSZ cermet anodes that have been exposed to different levels of phosphorus. For these efforts, electron dispersive spectroscopy (EDS) was used to identify Ni and YSZ, as well as the conversion of Ni to Ni_xP_y phases. Using the finite element analysis on RVEs of the structure, von Misses stresses in the Ni and YSZ phases of the structure were examined, along with their respective evolution. These stresses were the result of volumetric changes of Ni following phosphorous poisoning. Due to the strong interactions of Ni and P, contamination followed a wave-front type propagation with exposure and a unique stress evolution with time.

2.4. Molecular simulations

Molecular dynamics (MD) can provide a great deal of information about the rates of processes and the relaxation of materials. From a theoretical standpoint MD is rather straight-forward; Newton's laws of motion are applied to particles in the system, which correspond to atoms and molecules. Inter-particle interactions can take the form of electrostatic, Van der Wall's, and Lennard-Jones potentials, as well as the various modes of atomic and molecular motion. Many implementations use force fields to describe inter-atomic and molecular potentials that are either long-range or involve more complex processes that are dependent upon the atom/molecule's electronic structure. In terms of using MD methods to study functional heterogeneous structures, MD methods are quite suited to finite periodic regions descriptive of an interface or several unit cells of structure at this time due to their computational costs.

Among the more common approaches used within the SOFC community is a kinetic Monte Carlo (KMC) method. Prinz's group has made use of KMC for studying the mechanisms and properties of electrolyte materials [150,151]. These KMC studies require appropriate inter-atomic and inter-molecular descriptions, as discussed in the following section. In these studies, KMC has been used to develop an electrochemical impedance type simulation of the material's response and specifically details in regard to the oxygen diffusion at the space charge double layer at the electrode–electrolyte interfaces and the role of the electrolyte thickness [150]. This enabled experimental validation to impedance spectra. Information about the attributed energy barriers for electrolyte materials were required from density functional theory simulations. Using alternating potentials to represent the impedance response, low frequency oxide migration was found to be fast in the electrolyte and that there was an accumulation of oxide at the electrode–electrolyte interfaces forming a double layer and space charge region. Thicker electrolytes were found to require longer times to obtain the same double-layer characteristics. Only local ionic movement was recognized at higher frequencies. Double layer capacitances extracted from the simulations were found to be considerably larger than geometric capacitance contributions.

In a subsequent study using simulation methods to further understand impedance spectra, Prinz and coworkers used KMC to model vacancy migration in the solid electrolyte to show that the fluctuation dissipation theorem holds across all frequencies [151]. This study examined the effects of dopant concentrations in the oxide electrolyte. It was found that at infinite frequency, impedance decreases with increased doping. And at zero-frequency, dopant–vacancy interactions are dominant. Approaches to extend these efforts for the consideration of generalized surfaces and grain boundary contributions are discussed.

Goddard III and coworkers have performed MD based studies of oxygen ion transport in YSZ [152]. Reactive force fields have been developed and optimized, which are used to study oxygen ion diffusion in YSZ as a function of temperature. The results were validated with experimentally measured Arrhenius data, with high fidelity. This group notes that they are trying to develop an accurate description of oxide transport in YSZ so that force fields for various catalysts can be used to enable simulation of critical processes of these materials and interfaces and subsequent optimization at the interface-level.

Moving to the examination of the oxygen reduction reaction (ORR) in the SOFC cathode, Dunlap and corkers use KMC to study the mechanisms and rates [153–155]. First, KMC was used to study the LSM–YSZ interface and its affect on the ORR [153]. A sensitivity analysis using the ionic current density was used for this effort, and was found to be most sensitive to variations of the O^{2-} incorporation rate into the YSZ. This is a result of a large oxygen vacancy

diffusion barrier. Oxygen segregation-induced concentration gradients at the double layer were recognized as having key intrinsic properties that affect performance. In a subsequent study, Dunlap and coworkers also examine both the ORR with a Pt–YSZ cathode and the hydrogen oxidation reaction (HOR) of the Ni–YSZ anode [154]. This study identified oxygen incorporation into the YSZ electrolyte as rate limiting. Steps also of importance but will a smaller impact on the overall rate were identified as being the oxide ion transport in YSZ and oxygen spillover onto Ni for the HOR.

An interesting possibility for molecular level simulations that has not been extensively used in the context of heterogeneous SOFC is the use of such methods for examining the mechanical aspects of the constituent materials and interfaces. Sato et al. reported the use of MD, along with experimental efforts, to study the effects of compressive and tensile strain on the conductivity of Y_2O_3 doped CeO_2, where different amounts of dopant were considered [156]. These studies identified peak conductivity at a dopant concentration of approximately 20% Y_2O_3, which was in agreement for both simulation and experimental efforts. Elastic moduli were also in agreement and scaled inversely with conductivity.

Crack formation and propagation dynamics are topics that have been extensively studied at the atomic and molecular levels; however, do not appear to have ventured very far into the SOFC community [7,8]. The complex interactions of time/length scales and materials/structures involved presents a computational challenge for addressing these issues in the SOFC. As they become more tractable, such studies can provide details regarding the dynamics, pathways, and rates of fractures in complex systems and have specifically been applied to both brittle and ductile materials [8]. These approaches are of particular use for examination of highly strained and broken bonds, where quantum approaches are necessary for higher order accuracy of these processes [7].

2.5. Electronic structure and ab initio methods

The electronic structure of the atoms and molecules of the participating materials and interfaces can provide insight into the properties and nature of the system. Many of the configurations, properties, and mechanistic pathways may be addressed by calculation of the electronic structure of ensembles of atoms and molecules and the minimization of the energy associated with the structure/ensemble. As with molecular simulations, electronic structure calculations are typically too expensive to consider a large volume. They are better suited to extracting properties and details regarding the constituent materials, interfaces, configurations, energetic, and processes/pathways, which can be described in a periodic system. These facets are all important to interfacial phenomena like transport mechanisms/rates, reaction pathways, preferential adsorption sites/configuration, activation energies, mechanical properties, chemical stability, etc., which can calculated using minimum energy pathways [157].

Traditional DFT methods use a ground-state energy density that satisfies Schrödinger's equation to predict properties via treatment of the electronic density and ground state energy [55,157]. This may be achieved using a Kohn-Sham orbital, which express the ground-state energy as a function of the kinetic energy, exchange correlation energy, and interactions between the nuclei, electrons, and themselves. Tight binding methods may be used to separate contributions between core and valence electrons, the latter of which dominates covalently bonded systems which traditional DFT methods excel with [34]. The Kohn-Sham orbital requires a suitable exchange correlation energy term. Local density (LDA) and generalized gradient approximations (GGA) are often used. The GGA is noted for its balance of cost and providing qualitatively correct chemical properties, making it a method of choice for studying topics like heterogeneous catalysis [1]. Suitable, functional forms are required for the generalized gradient approximation, such as Perdew-Burke-Ernzerhof (PBE) and Perdew-Wang 91 (PW91).

In the SOFC community, a number of research groups have been using DFT-based methods to understand material, interface, and nanostructure properties as well as physical/chemical pathways. In terms of the conductivity of the common YSZ electrolyte material, Pornprasertsuk et al. used a DFT method using LDA and gradient correction with kinetic Monte Carlo to study the oxygen vacancy diffusion mechanism [158]. The effect of dopant concentration on conductivity was examined, where DFT provided the energy barriers along the minimum energy path for a vacancy to migrate/diffuse. Traditional material defect theory would suggest that conductivity should continue to increase with dopant concentration; however, it has long been recognized that the conductivity no longer increases once approximately 8 mol% Y_2O_3 is reached. Pornprasertsuk et al. identified the migration energy needed to traverse two adjacent tetrahedral containing the Zr–Y and Y–Y common edge as the root of this limitation [158]. Experimental and simulated conductivity versus dopant concentration trends were in strong accord.

Adsorption, dissociation, and pathways associated with catalytic and electrocatalytic processes supported by the heterogeneous electrode structures were explored by Rosmeisl and Bessler, whom used plane-wave DFT with GGA to calculate the stability of H, O, and OH radicals on Mn, Fe, Co, Ni, Cu, Ru, Rh, Pd, Ag, Pt, and Au [159]. These materials were treated as candidate anode electrocatalyst materials and were interfaced with YSZ so that electrochemical oxidation pathways could be examined via energy minimization. Oxygen spillover was identified as a dominant pathway, with the electrocatalytic activity linked to the binding affinities of the reactive intermediates. The electrocatalytic activity, defined as the change in free energy for the rate determining step, was found to scale with the experimentally determined binding energy for the various catalysts with Ni sitting atop the volcano plot [159].

Like Rosmeisl and Bessler, Shishkin and Ziegler [160] and Ingram and Linic [161] used similar approaches to study the activity of various materials for direct hydrocarbon oxidation. Shishkin and Ziegler used a DFT algorithm employing a PBE based exchange-correlation functional using spin-polarized calculations and a projected augmented wave method to study the oxidation of H_2, CH_4, and CO at the Ni/YSZ interface (i.e., TPB) with a focus on the charge transfer processes. In this effort, Shishkin and Ziegler noted that H_2 and CH_4 have relatively large adsorption activation barriers, whereas CO is favorable but endothermic. Oxygen spillover from YSZ is suggested as being dominant, but it is further suggested that some H-spillover from Ni to YSZ may compliment this process. Further, it is observed that H can oxidize an O-enriched surface, but that O-enriched YSZ is less active near Ni than an infinite YSZ surface [160]. Ingram and Linic used a plane wave basis set based DFT with electron exchange and correlation being described by the PW91 function with a GGA to study various metal catalysts, and how they behave in the presence of hydrocarbons [161]. They note that noble metals are relatively inert to coking because they do not activate C–H bonds and that active metals, such as W, Fe, and Mo are poisoned by oxygen and carbon. This implies that metals like Co, Ru, Ir, Rh, and Ni offer the optimal performance because they can activate CH_4 for charge transfer while not necessarily oxidizing. These metals still suffer from C-poisoning, depending upon the C/O ratio due to the formation of C–O rather than C–C bonds [161].

Besides the anodic processes, the oxygen reduction reaction in the cathode has also extensively been studied, as evident by the review by Choi et al., who highlight the challenges of the surface and interface models for the junction of the electrode and electrolytic materials [157]. In this review one of the topics examined was the adsorption sites and configurations for perovskite cathode materials, as well as the oxygen incorporation step. A study

by Mastrikov et al., whom used DFT calculations with exchange correlations using a GGA with a PW91 function and plane wave basis set, studied the mechanism of oxygen incorporation into $(La_{1-x}Sr_x)MnO_{3-\delta}$ [162]. As a part of this effort, MnO_2 (0 0 1) was identified as the most stable surface termination for fuel cell conditions. Mechanistically, the rate determining step was identified as the surface oxygen vacancy encountering an adsorbed O^- via activated surface diffusion of the vacancy. This points toward the need for a higher surface vacancy concentration and mobility. As a part of these efforts, oxygen adsorbates were found to be rather low, which was explained by negative adsorption entropy and electrostatic repulsion, despite the exothermic formation of O_2^-, O_2^{2-}, and O^- on Mn.

Another prominent concern with the materials used in the SOFC's heterogeneous materials is their stability in the presence of poisons and contaminants. In an attempt to address the stability and degradation mechanisms of Ni in the presence of carbonaceous fuels, Nikolla et al. used DFT with the exchange correlation formulated using a GGA with a PW91 function set [163]. They identified that alloying the Ni surface can promote the oxidation of C atoms, rather than allowing the formation of strong C–C bonds, which have a lower driving force and thus permit the nucleation of C atoms on low-coordinated Ni sites. In conjunction with experimental efforts, a Sn/Ni alloy was shown to improve stability to carbon and adsorption relative to Ni (1 1 1), in the presence of methane, propane, and isooctane with a steam to carbon ratio of 1.5. These demonstrations experimentally exhibited hundreds of hours of stability. Galea et al. performed similar simulations on Ni and Cu (1 1 1) and (2 1 1), as well as Cu–Ni and Cu–Co alloys in the presence of CH_4 [164]. They found that C adsorbs strongly onto the Ni (2 1 1) surface and grows graphitic carbon over the terrace; however, Cu was found to have a very high thermodynamic and kinetic barrier to CH_4 dissociation. This dissociation barrier restricts breakdown and provides opportunities for direct electrochemical oxidation. The Cu–Ni and Cu–Co alloys showed that Ni and Co has little effect on surface Cu and that stability is limited by the Cu enrichment of the alloy surface.

Besides carbon, sulfur is also a particularly challenging contaminant for the SOFC anode. Wang and Liu used DFT with the exchange correlation treated using a GGA with the PBE function to study the regeneration of a Ni catalyst surface with O_2 and H_2O after the catalyst was exposed to S [41]. The study found that both O_2 and H_2O were practical for sulfur removal; however, H_2O was suggested as the better choice because of its ability to remove sulfur over a wider range of pressures without oxidizing the Ni. The study considered the removal and adsorption of sulfur, as well as the oxidation of the Ni surface to form NiO.

Reduction and re-oxidation (redox) instability in the SOFC has been widely documented as leading to irreversible degradation, typically through mechanical changes in the structure. Coarsening and irreversible changes have been suggested as the culprit; however, details of the exact mechanisms remain elusive. In a study by Jeangros et al., DFT using GGA with PBE exchange and correlation has been used to confirm *in situ* high resolution environmental transmission electron microscope (HR-TEM) reduction and re-oxidation (redox) cycle studies of the Ni–YSZ cermet SOFC anode [26]. This investigation linked these experiments to DFT based studies of the pathways for the reduction and re-oxidation of the Ni/NiO in the Ni–YSZ cermet anode. For this effort, vacancies near the Ni–YSZ interface were introduced with the nudged elastic band (NEB) approach. Experimentally, reduction showed the transformation of NiO grains to metallic Ni, leaving a nanoporous structure. The formation of additional Ni nanoparticles was also observed. Jeangros et al. suggested that the reduction process initiated with the reduction of NiO at the NiO/YSZ interface followed by that of the free NiO surfaces. The NEB calculations confirmed this behavior as it showed that the relative defect energy reduced when the oxygen was incorporated into the YSZ, which was related to relaxation in strain with the vacancy in the NiO. This led to a two step pathway being proposed, in which oxygen ions are transferred from NiO to YSZ, which subsequently desorbs as water. The first involved the transfer of the oxygen to the YSZ at the NiO/YSZ interface, followed by the reduction of the oxygen in the YSZ with hydrogen, forming water that subsequently desorbs. The authors noted that a complementary mechanism of hydrogen adsorbing onto the Ni adjacent to oxygen vacancies may allow water to desorb directly at the NiO/Ni interface and allow NiO reduction to continue toward the center of the grain, which is consistent with the direct reduction of the free Ni/NiO surface [26].

While GGA based DFT approaches have been mainstays, DFT + U and similar hybrid methods are becoming more prominent because they are becoming more robust and permit additional relevant processes and materials to be studied [1,34]. Huang and Carter note that hybrid schemes like DFT + U provide less expensive calculations for materials involving mixed electron distributions and highly correlated materials [1,34]. This specifically relates to structures and materials incorporating transition metal oxides and sulfides, which are prevalent in the SOFC materials and processes. The improvement of DFT + U methods results from its exact incorporation of the exchange process.

An example of the use of the DFT + U framework is a work by Chen et al., whom used the method to study the sulfur tolerance of Ceria (CeO_2) [165]. The study required DFT + U to appropriately correct for the on-site coulomb repulsion of the Ce_{4f} state localizations. The general calculations used GGA based DFT with PW91 exchange-correlation functional. This study examined the interactions of hydrogen sulfide (H_2S) with CeO_2 (1 1 1), with H_2S, HS, and S intermediates, which were produced as a result of low dehydrogenation barriers. Adsorption sites were explored, finding a variety of bridging sites. Dehydrogenated surface adsorbates were further shown to react with available oxygen anions under operational conditions, with an SO_2 forming pathway being the most likely [165]. While not directly compared, surface vibrational spectra were calculated as a part of this effort so that they could be compared to experimental measurements in future studies.

Another DFT + U study was reported by Shishkin and Ziegler to examine the chemical properties of Ni/Ceria (CeO_2) and Ni/CeO_2/YSZ SOFC anodes [166]. DFT + U was required because of the coulomb repulsion of the Ce_{4f} electrons. For this effort, charge localization resulting from vacancy formation was examined, as they relate to the adsorption and reaction of H_2 and CH_4 fuels on the ceria surface. The adsorption of H_2 and CH_4 onto the Ni/CeO_2 surface approaches those of pure CeO_2, suggesting similar mechanisms and rates. Both hydrogen and oxygen spillover pathways were examined, where oxygen spillover onto Ni was both significant and suggestive of the higher coking tolerance. During oxidation, a ceria surface vacancy formation resulted in the transfer of a small amount of charge to the Ni. This is different than Ni/YSZ where the valance band structure dictates that it is energetically favorable to transfer the electronic charge to the Ni. Still, the more prominent pathway was the oxidation of the fuel at the CeO_2 surface [166].

Recently, Carter et al. applied DFT + U methods to study oxide ion conductivity in perovskite-type transition metal oxides $LaMO_3$ (M = Cr, Mn, Fe, Co) for SOFC cathode materials [168] and Sr_2FeMoO_6, mixed ionic and electronic conductors proposed as electrodes for SOFC applications [169]. Bulk oxygen vacancy formation, which is a key factor for the oxide ion bulk diffusion process, was carefully examined for various material compositions. Important design principles were derived based on easily measurable or computable properties.

Several additional methods, which have not been extensively used in the SOFC community, include quantum Monte Carlo (QMC) and AIMD methods. QMC is very accurate for highly correlated

systems, but remains expensive and difficult to implement [1,34]. Computational expense also limits AIMD based methods, which link molecular mechanics and electronic structure calculations [1,34,55]. AIMD may be considered a part of a broader class of embedded cluster methods, which try to incorporate longer range effects by coupling the domain with more general theory via carefully selected partitioning. However, this becomes difficult as size effects become important. Certainly, AIMD has had limited applicability in the SOFC community to date because of the time and length scales required to perform analysis at SOFC conditions with consistent calculations of the electronic structure.

3. Conclusions and outlook

Over the course of this review, a variety of studies that have explored unique aspects and scales of the SOFC system, operation, structure, chemical and physical processes, and degradation/evolution have been highlighted. Many of these studies, which are a sampling of those within the community, have taken unique aspects to understand processes in the SOFC. Individually, each of the methods presented is capable of providing valuable information regarding the properties, performance, structure, and interactions within the heterogeneous structures comprising the electrode structures of the SOFC, which should improve with advancements in computational facilities and theory/algorithms.

These individual incremental advances hold tremendous value; however, more substantial advances may come from the coupling of these approaches and scales to ascertain more of the multi-scaled nature of the heterogeneous SOFC materials. Incorporating the strengths of these individual methods, time and length scale coupling, along with those of the unique physical, chemical and mechanical processes that constitutes the materials' behavior should be able to be understood at unprecedented levels. This includes predictive capabilities for never-before manufactured materials [1]. Whether automated or with explicit human interaction, this coupling should allow inter-dependencies of the numerous variables involved in the properties and function of the heterogeneous material system to be systematically understood. A key aspect to realizing such a robust level of modeling and simulation is the complementary development of improved experimental capabilities; specifically those that can provide new levels of detail regarding the atomic, chemical, structural, and mechanical interactions within the cell as are related to its composition and function. These tools can provide unique opportunities to better define the system and conditions, as well as provide an effective means for validation.

With ongoing experimental and modeling/simulation advancements, the community seems poised to translate individual insights gained from systematic studies to more of a robust approach which considering a wider breadth of scales, processes, and interactions within the system. This type of capability can present both unprecedented challenges and opportunities to systematically understand the SOFC and transition from more Edisonian approaches to the methodical engineering of advanced materials, structures, and components that form these multiscaled, multifunctional, heterogenerous functional materials (HeteroFoaMs).

Acknowledgments

WKSC gratefully acknowledges financial support from the Energy Frontier Research Center on Science Based Nano-Structure Design and Synthesis of Heterogeneous Functional Materials for Energy Systems (HeteroFoaM Center) funded by the U.S. Department of Energy, Office of Science, Office of Basic Energy Sciences (Award DE-SC0001061). KNG gratefully acknowledges that this effort was supported, in part, by an appointment to the U.S. Army Research Laboratory Postdoctoral Fellowship Program administered by the Oak Ridge Associated Universities through a contract with the U.S. Army Research Laboratory with financial support from the U.S. Department of the Army and the U.S. Army Materiel Command. The authors are grateful to Prof. Emily A. Carter at Princeton University, Prof. Kenneth L. Reifsnider at the University of South Carolina, Prof. Anil V. Virkar at the University of Utah, and Dr. Deryn Chu of the U.S. Army Research Laboratory for invaluable discussion and support.

References

[1] E.A. Carter, Science 321 (2008) 800–803.
[2] H.L. Tuller, J. Electroceram. 4 (1999) 33–40.
[3] H.L. Tuller, Solid State Ionics 131 (2000) 143–157.
[4] J.O.M. Bockris, A.K.N. Reddy, M. Gamboa-Aldeco, Modern electrochemistry 2A: Fundamentals of Electrodics, Kluwer Academic, New York, 2002.
[5] R.I. Masel, Chemical Kinetics and Catalysis, Wiley-Interscience, New York, 2001.
[6] R.I. Masel, Principles of Adsorption and Reaction on Solid Surfaces, Wiley, New York, 1996.
[7] F.F. Abraham, Nucl. Instrum. Methods B 180 (2001) 72–76.
[8] F.F. Abraham, D. Brodbeck, W.E. Rudge, X. Xu, J. Mech. Phys. Solids 45 (1997) 1595–1619.
[9] P.D. Zavattieri, H.D. Espinosa, Acta Mater. 49 (2001) 4291–4311.
[10] L. Bouhala, S. Belouettar, A. Makradi, Y. Remond, Mater. Des. 31 (2010) 1033–1041.
[11] N. Nguyen, B.J. Koeppel, S. Ahzi, M.A. Khaleel, P. Singh, J. Am. Ceram. Soc. 89 (2006) 1358–1368.
[12] R.B. Bird, W.E. Stewart, E.N. Lightfoot, Transport Phenomena, 2nd ed., J. Wiley, New York, 2002.
[13] J.O. Hirschfelder, C.F. Curtiss, R.B. Bird, Molecular Theory of Gases and Liquids, Wiley, New York, 1964.
[14] M. Kaviany, Heat Transfer Physics, Cambridge University Press, Cambridge, 2008.
[15] E.A. Mason, A.P. Malinauskas, R.B. Evans, J. Chem. Phys. 46 (1967), 3199-&.
[16] G. Ehrlich, K. Stolt, Annu. Rev. Phys. Chem. 31 (1980) 603–637.
[17] K. Reifsnider, X. Huang, G. Ju, R. Solasi, J. Mater. Sci. 41 (2006) 6751–6759.
[18] J. Maier, Nat. Mater. 4 (2005) 805–815.
[19] X. Guo, J. Maier, J. Electrochem. Soc. 148 (2001) E121–E126.
[20] H. Yokokawa, H.Y. Tu, B. Iwanschitz, A. Mai, J. Power Sources 182 (2008) 400–412.
[21] L. Ratke, P.W. Voorhees, Growth and Coarsening: Ostwald Ripening in Material Processing, Springer, Berlin; New York, 2002.
[22] T. Klemenso, C.C. Appel, M. Mogensen, Electrochem. Solid State Lett. 9 (2006) A403–A407.
[23] M. Pihlatie, A. Kaiser, P.H. Larsen, M. Mogensen, J. Electrochem. Soc. 156 (2009) B322–B329.
[24] M. Pihlatie, A. Kaiser, M. Mogensen, Solid State Ionics 180 (2009) 1100–1112.
[25] D. Sarantaridis, A. Atkinson, Fuel Cells 7 (2007) 246–258.
[26] Q. Jeangros, A. Faes, J.B. Wagner, T.W. Hansen, U. Aschauer, J. Van herle, A. Hessler-Wyser, R.E. Dunin-Borkowski, Acta Mater. 58 (2010) 4578–4589.
[27] H. Kishimoto, T. Horita, K. Yamaji, M.E. Brito, Y.P. Xiong, H. Yokokawa, J. Electrochem. Soc. 157 (2010) B802–B813.
[28] H. Yokokawa, T. Horita, N. Sakai, K. Yamaji, M.E. Brito, Y.P. Xiong, H. Kishimoto, Solid State Ionics 177 (2006) 3193–3198.
[29] K. Ogasawara, H. Kameda, Y. Matsuzaki, T. Sakurai, T. Uehara, A. Toji, N. Sakai, K. Yamaji, T. Horita, H. Yokokawa, J. Electrochem. Soc. 154 (2007) B657–B663.
[30] A. Nakajo, C. Stiller, G. Harkegard, O. Bolland, J. Power Sources 158 (2006) 287–294.
[31] A. Nakajo, Z. Wuillemin, J. Van herle, F. Daniel, J. Power Sources 193 (2009) 216–226.
[32] A. Nakajo, Z. Wuillemin, J. Van herle, D. Favrat, J. Power Sources 193 (2009) 203–215.
[33] X. Zhao, F.H. Wang, X. Wang, Z.Q. Liu, J. Inorg. Mater. 26 (2011) 393–397.
[34] P. Huang, E.A. Carter, Annu. Rev. Phys. Chem. 59 (2008) 261–290.
[35] J. Maier, Prog. Solid State Chem. 23 (1995) 171–263.
[36] J. Maier, Int. J. Mater. Res. 99 (2008) 24–25.
[37] F. Zhao, A.V. Virkar, J. Power Sources 195 (2010) 6268–6279.
[38] I. Lubomirsky, J. Fleig, J. Maier, J. Appl. Phys. 92 (2002) 6819–6827.
[39] E.M. Ryan, A.M. Tartakovsky, K.P. Recknagle, M.A. Khaleel, C. Amon, J. Power Sources 196 (2011) 287–300.
[40] M.R. Pillai, I. Kim, D.M. Bierschenk, S.A. Barnett, J. Power Sources 185 (2008) 1086–1093.
[41] J.-H. Wang, M. Liu, J. Power Sources 176 (2008) 23–30.
[42] A. Utz, K.V. Hansen, K. Norrman, E. Ivers-Tiffee, M. Mogensen, Solid State Ionics 183 (2011) 60–70.
[43] A. Hauch, M. Mogensen, Solid State Ionics 181 (2010) 745–753.
[44] S.D. Ebbesen, C. Graves, A. Hauch, S.H. Jensen, M. Mogensen, J. Electrochem. Soc. 157 (2010) B1419–B1429.

[45] M.S. Schmidt, K.V. Hansen, K. Norrman, M. Mogensen, Solid State Ionics 179 (2008) 1436–1441.
[46] K. Norrman, K.V. Hansen, M. Mogensen, J. Eur. Ceram. Soc. 26 (2006) 967–980.
[47] K.V. Hansen, K. Norrman, M. Mogensen, J. Electrochem. Soc. 151 (2004) A1436–A1444.
[48] Y.L. Liu, S. Primdahl, M. Mogensen, Solid State Ionics 161 (2003) 1–10.
[49] C.C. Xu, J.W. Zondlo, M.Y. Gong, X.B. Liu, J. Power Sources 196 (2011) 116–125.
[50] C.C. Xu, J.W. Zondlo, M.Y. Gong, F. Elizalde-Blancas, X.B. Liu, I.B. Celik, J. Power Sources 195 (2010) 4583–4592.
[51] A. Martinez, K. Gerdes, R. Gemmen, J. Poston, J. Power Sources 195 (2010) 5206–5212.
[52] M.C. Tucker, H. Kurokawa, C.P. Jacobson, L.C. De Jonghe, S.J. Visco, J. Power Sources 160 (2006) 130–138.
[53] J.Y. Kim, V.L. Sprenkle, N.L. Canfield, K.D. Meinhardt, L.A. Chick, J. Electrochem. Soc. 153 (2006) A880–A886.
[54] W. Liu, X. Sun, L.R. Pederson, O.A. Marina, M.A. Khaleel, J. Power Sources 195 (2010) 7140–7145.
[55] J. Kohanoff, Electronic Structure Calculations for Solids and Molecules: Theory and Computational Methods, Cambridge University Press, Cambridge, UK, 2006.
[56] C.J. Cramer, Essentials of Computational Chemistry: Theories & Models, Wiley, New York, 2002.
[57] L.Q. Chen, Annu. Rev. Mater. Res. 32 (2002) 113–140.
[58] W.L. George, J.A. Warren, J. Comput. Phys. 177 (2002) 264–283.
[59] C.L. Martin, D. Bouvard, S. Shima, J. Mech. Phys. Solids 51 (2003) 667–693.
[60] S. Succi, The Lattice Boltzmann Equation for Fluid Dynamics and Beyond, Clarendon Press, Oxford, 2001.
[61] M.C. Sukop, D.T. Thorne, Lattice Boltzmann Modeling: An Introduction for Geoscientists and Engineers, Springer, Berlin, 2006.
[62] S. Chen, G.D. Doolen, Annu. Rev. Fluid Mech. 30 (1998) 329–364.
[63] F. Toschi, S. Succi, Europhys. Lett. 69 (2005) 549–555.
[64] A.S. Joshi, A.A. Peracchio, K.N. Grew, W.K.S. Chiu, J. Phys. D 40 (2007) 7593–7600.
[65] R. Zhang, X. Shan, H. Chen, Phys. Rev. E 74 (2006) 046703.
[66] S.V. Patankar, Numerical Heat Transfer and Fluid Flow, McGraw-Hill, Washington, 1980.
[67] I.M. Smith, D.V. Griffiths, Programming the Finite Element Method, 4th ed., Wiley, Hoboken, NJ, 2004.
[68] K.P. Recknagle, R.E. Williford, L.A. Chick, D.R. Rector, M.A. Khaleel, J. Power Sources 113 (2003) 109–114.
[69] M.A. Khaleel, Z. Lin, P. Singh, W. Surdoval, D. Collin, J. Power Sources 130 (2004) 136–148.
[70] K.P. Recknagle, E.M. Ryan, B.J. Koeppel, L.A. Mahoney, M.A. Khaleel, J. Power Sources 195 (2010) 6637–6644.
[71] S.C. DeCaluwe, H. Zhu, R.J. Kee, G.S. Jackson, J. Electrochem. Soc. 155 (2008) B538–B546.
[72] H. Zhu, R.J. Kee, J. Electrochem. Soc. 155 (2008) B715–B729.
[73] D. Chen, Z. Lin, H. Zhu, R.J. Kee, J. Power Sources 191 (2009) 240–252.
[74] W.G. Bessler, Solid State Ionics 176 (2005) 997–1011.
[75] W.G. Bessler, J. Electrochem. Soc. 154 (2007) B1186–B1191.
[76] W.G. Bessler, S. Gewies, M. Vogler, Electrochim. Acta 53 (2007) 1782–1800.
[77] S. Gewies, W.G. Bessler, J. Electrochem. Soc. 155 (2008) B937–B952.
[78] M. Vogler, A. Bieberle-Hutter, L. Gauckler, J. Warnatz, W.G. Bessler, J. Electrochem. Soc. 156 (2009) B663–B672.
[79] H. Zhu, R.J. Kee, J. Power Sources 117 (2003) 63–74.
[80] H. Zhu, R.J. Kee, V.M. Janardhanan, O. Deutschmann, D.G. Goodwin, J. Electrochem. Soc. 152 (2005) A2427–A2440.
[81] G.M. Goldin, H. Zhu, R.J. Kee, D. Bierschenk, S.A. Barnett, J. Power Sources 187 (2009) 123–135.
[82] H. Zhu, R.J. Kee, J. Power Sources 169 (2007) 315–326.
[83] H. Zhu, R.J. Kee, J. Electrochem. Soc. 153 (2006) A1765–A1772.
[84] H. Zhu, A.M. Colclasure, R.J. Kee, Y. Lin, S.A. Barnett, J. Power Sources 161 (2006) 413–419.
[85] G.K. Gupta, J.R. Marda, A.M. Dean, A.M. Colclasure, H. Zhu, R.J. Kee, J. Power Sources 162 (2006) 553–562.
[86] M. Pillai, Y. Lin, H. Zhu, R.J. Kee, S.A. Barnett, J. Power Sources 195 (2010) 271–279.
[87] E.S. Hecht, G.K. Gupta, H.Y. Zhu, A.M. Dean, R.J. Kee, L. Maier, O. Deutschmann, Appl. Catal. A 295 (2005) 40–51.
[88] M.R. Pillai, Y. Jiang, N. Mansourian, I. Kim, D.M. Bierschenk, H. Zhu, R.J. Kee, S.A. Barnett, Electrochem. Solid State Lett. 11 (2008) B174–B177.
[89] G. Anandakumar, J.-H. Kim, Int. J. Fract. 164 (2010) 31–55.
[90] G. Anandakumar, N. Li, A. Verma, P. Singh, J.-H. Kim, J. Power Sources 195 (2010) 6659–6670.
[91] L.-K. Chiang, H.-C. Liu, Y.-H. Shiu, C.-H. Lee, R.-Y. Lee, J. Power Sources 195 (2010) 1895–1904.
[92] L. Liu, G.-Y. Kim, A. Chandra, J. Power Sources 195 (2010) 2310–2318.
[93] A. Selimovic, M. Kemm, T. Torisson, M. Assadi, J. Power Sources 145 (2005) 463–469.
[94] C.-K. Lin, L.-H. Huang, L.-K. Chiang, Y.-P. Chyou, J. Power Sources 192 (2009) 515–524.
[95] M.H. Pihlatie, H.L. Frandsen, A. Kaiser, M. Mogensen, J. Power Sources 195 (2010) 2677–2690.
[96] H. Yakabe, T. Ogiwara, M. Hishinuma, I. Yasuda, J. Power Sources 102 (2001) 144–154.
[97] J. Villanova, O. Sicardy, R. Fortunier, J.S. Micha, P. Bleuet, Nucl. Instrum. Methods B 268 (2010) 282–286.
[98] R. Rengaswamy, D. Bhattacharyya, Ind. Eng. Chem. Res. 48 (2009) 6068–6086.
[99] R. Bove, S. Ubertini, J. Power Sources 159 (2006) 543–559.
[100] S.C. Singhal, K. Kendall, High Temperature Solid Oxide Fuel Cells: Fundamentals, Design, and Applications, Elsevier, Burlington, 2003.
[101] P. Costamagna, P. Costa, V. Antonucci, Electrochim. Acta 43 (1998) 375–394.
[102] P. Costamagna, P. Costa, E. Arato, Electrochim. Acta 43 (1998) 967–972.
[103] S.H. Chan, Z.T. Xia, J. Electrochem. Soc. 148 (2001) A388–A394.
[104] P. Costamagna, M. Panizza, G. Cerisola, A. Barbucci, Electrochim. Acta 47 (2002) 1079–1089.
[105] C.W. Tanner, K.-Z. Fung, A.V. Virkar, J. Electrochem. Soc. 144 (1997) 21–30.
[106] A.V. Virkar, J. Chen, C.W. Tanner, J.-W. Kim, Solid State Ionics 131 (2000) 189–198.
[107] G.J. Nelson, A.A. Peracchio, W.K.S. Chiu, J. Power Sources 196 (2011) 4695–4704.
[108] S. Sunde, J. Electrochem. Soc. 142 (1995) L50–L52.
[109] S. Sunde, J. Electrochem. Soc. 143 (1996) 1123–1132.
[110] S. Sunde, J. Electrochem. Soc. 143 (1996) 1930–1939.
[111] J. Deseure, Y. Bultel, L.C.R. Schneider, L. Dessemond, C. Martin, J. Electrochem. Soc. 154 (2007) B1012–B1016.
[112] L.C.R. Schneider, C.L. Martin, Y. Bultel, D. Bouvard, E. Siebert, Electrochim. Acta 52 (2006) 314–324.
[113] L.C.R. Schneider, C.L. Martin, Y. Butlel, L. Dessemond, D. Bouvard, Electrochim. Acta 52 (2007) 3190–3198.
[114] J. Sanyal, G.M. Goldin, H. Zhu, R.J. Kee, J. Power Sources 195 (2010) 6671–6679.
[115] C.L.Y. Yeong, S. Torquato, Phys. Rev. E 57 (1998) 495–506.
[116] S. Torquato, S. Hyun, A. Donev, J. Appl. Phys. 94 (2003) 5748–5755.
[117] N. Sheehan, S. Torquato, J. Appl. Phys. 89 (2001) 53–60.
[118] Y. Jiao, F.H. Stillinger, S. Torquato, Phys. Rev. E 76 (2007) 031110.
[119] Y. Jiao, F.H. Stillinger, S. Torquato, Phys. Rev. E 77 (2008) 031135.
[120] X. Guo, J. Maier, Adv. Mater. 21 (2009) 2619–2631.
[121] J. Jamnik, J. Maier, Solid State Ionics 119 (1999) 191–198.
[122] J. Maier, Solid State Ionics 157 (2003) 327–334.
[123] J. Maier, Solid State Ionics 175 (2004) 7–12.
[124] J. Maier, Solid State Ionics 154–155 (2002) 291–301.
[125] J.-S. Lee, J. Jamnik, J. Maier, Monatsh. Chem. 140 (2009) 1113–1119.
[126] J. Garcia-Barriocanal, A. Rivera-Calzada, M. Varela, Z. Sefrioui, E. Iborra, C. Leon, S.J. Pennycook, J. Santamaria, Science 321 (2008) 676–680.
[127] A.S. Joshi, A.A. Peracchio, K.N. Grew, W.K.S. Chiu, J. Phys. D 40 (2007) 2961–2971.
[128] A.S. Joshi, K.N. Grew, A.A. Peracchio, W.K.S. Chiu, J. Power Sources 164 (2007) 631–638.
[129] W.K.S. Chiu, A.S. Joshi, K.N. Grew, Eur. Phys. J. Spec. Top. 171 (2009) 159–165.
[130] A.S. Joshi, K.N. Grew, J. Izzo, R. John, A.A. Peracchio, W.K.S. Chiu, ASME J. Fuel Cell Sci. Technol. 7 (2010) 011006.
[131] J.R. Izzo Jr., A.S. Joshi, K.N. Grew, W.K.S. Chiu, A. Tkachuk, S.H. Wang, W. Yun, J. Electrochem. Soc. 155 (2008) B504–B508.
[132] K.N. Grew, A.S. Joshi, A.A. Peracchio, W.K.S. Chiu, J. Power Sources 195 (2010) 2331–2345.
[133] K.N. Grew, Y.S. Chu, J. Yi, A.A. Peracchio, J.R. Izzo Jr., Y. Hwu, F. De Carlo, W.K.S. Chiu, J. Electrochem. Soc. 157 (2010) B783–B792.
[134] K.N. Grew, A.A. Peracchio, W.K.S. Chiu, J. Power Sources 195 (2010) 7943–7958.
[135] K.N. Grew, A.S. Joshi, W.K.S. Chiu, Fuel Cells 10 (2011) 031001.
[136] P. Asinari, M.C. Quaglia, M.R. von Spakovsky, B.V. Kansula, J. Power Sources 170 (2007) 359–375.
[137] K.N. Grew, A.A. Peracchio, A.S. Joshi, J. Izzo, R. John, W.K.S. Chiu, J. Power Sources 195 (2010) 7930–7942.
[138] N. Shikazono, D. Kanno, K. Matsuzaki, H. Teshima, S. Sumino, N. Kasagi, J. Electrochem. Soc. 157 (2010) B665–B672.
[139] S.G. Kim, Acta Mater. 55 (2007) 6513–6525.
[140] T. Kitashima, H. Harada, Acta Mater. 57 (2009) 2020–2028.
[141] C. Shen, Q. Chen, Y.H. Wen, J.P. Simmons, Y. Wang, Scripta Mater. 50 (2004) 1023–1028.
[142] Y.H. Wen, B. Wang, J.P. Simmons, Y. Wang, Acta Mater. 54 (2006) 2087–2099.
[143] J.H. Kim, W.K. Liu, C. Lee, Comput. Mech. 44 (2009) 683–703.
[144] H.Y. Chen, H.C. Yu, J.S. Cronin, J.R. Wilson, S.A. Barnett, K. Thornton, J. Power Sources 196 (2011) 1333–1337.
[145] J.R. Wilson, W. Kobsiriphat, R. Mendoza, H.Y. Chen, J.M. Hiller, D.J. Miller, K. Thornton, P.W. Voorhees, S.B. Adler, S.A. Barnett, Nat. Mater. 5 (2006) 541–544.
[146] J.R. Wilson, A.T. Duong, M. Gameiro, H.Y. Chen, K. Thornton, D.R. Mumm, S.A. Barnett, Electrochem. Commun. 11 (2009) 1052–1056.
[147] J.R. Wilson, M. Gameiro, K. Mischaikow, W. Kalies, P.W. Voorhees, S.A. Barnett, Microsc. Microanal. 15 (2009) 71–77.
[148] J.R. Wilson, J.S. Cronin, A.T. Duong, S. Rukes, H.Y. Chen, K. Thornton, D.R. Mumm, S. Barnett, J. Power Sources 195 (2010) 1829–1840.
[149] H.D. Espinosa, P.D. Zavattieri, Mech. Mater. 35 (2003) 365–394.
[150] R. Pornprasertsuk, J. Cheng, H. Huang, F.B. Prinz, Solid State Ionics 178 (2007) 195–205.
[151] E. Lee, F.B. Prinz, W. Cai, Electrochem. Commun. 12 (2010) 223–226.
[152] A.C.T. van Duin, B.V. Merinov, S.S. Jang, W.A. Goddard III, J. Phys. Chem. A 112 (2008) 3133–3140.
[153] K.C. Lau, C.H. Turner, B.I. Dunlap, Chem. Phys. Lett. 471 (2009) 326–330.

[154] X. Wang, K.C. Lau, C.H. Turner, B.I. Dunlap, J. Power Sources 195 (2010) 4177–4184.
[155] K.C. Lau, C.H. Turner, B.I. Dunlap, Solid State Ionics 179 (2008) 1912–1920.
[156] K. Sato, K. Suzuki, J. Yashiro, T. Kawada, H. Yugami, T. Hashida, A. Atkinson, J. Mizusaki, Solid State Ionics 180 (2009) 1220–1225.
[157] Y.M. Choi, D.S. Mebane, J.-H. Wang, M. Liu, Top. Catal. 46 (2007) 386–401.
[158] R. Pornprasertsuk, P. Ramanarayanan, C.B. Musgrave, F.B. Prinz, J. Appl. Phys. 98 (2005) 103513.
[159] J. Rossmeisl, W.G. Bessler, Solid State Ionics 178 (2008) 1694–1700.
[160] M. Shishkin, T. Ziegler, J. Phys. Chem. C 113 (2009) 21667–21678.
[161] D.B. Ingram, S. Linic, J. Electrochem. Soc. 156 (2009) B1457–B1465.
[162] Y.A. Mastrikov, R. Merkle, E. Heifets, E.A. Kotomin, J. Maier, J. Phys. Chem. C 114 (2010) 3017–3027.
[163] E. Nikolla, J. Schwang, S. Linic, J. Catal. 250 (2007) 85–93.
[164] N.M. Galea, D. Knapp, T. Ziegler, J. Catal. 247 (2007) 20–33.
[165] H.T. Chen, Y.M. Choi, M.L. Liu, M.C. Lin, J. Phys. Chem. C 111 (2007) 11117–11122.
[166] M. Shishkin, T. Ziegler, J. Phys. Chem. C 114 (2010) 21411–21416.
[167] W.K.S. Chiu, A.V. Virkar, F. Zhao, K.L. Reifsnider, G.J. Nelson, F. Rabbi, Q. Liu, HeteroFoaMs: electrode modeling in nano-structured heterogeneous materials for energy systems, J. Fuel Cell Sci. Tech. (2011), doi:10.1115/1.4005142.
[168] M. Pavone, A.M. Ritzmann, E.A. Carter, Energy Environ. Sci. (2011), doi:10.1039/c1ee02377b.
[169] A.B. Muñoz-García, M. Pavone, E.A. Carter, Chem. Mater. 23 (2011) 4525–4536.